JOURNAL OF SPACECRAFT AND ROCKETS
Vol. 31, No. 2, March–April 1994

NASA/National Space Science Data Center Trapped Radiation Models

John D. Gaffey Jr.* and Dieter Bilitza†
Hughes STX, Greenbelt, Maryland 20770

The National Space Science Data Center (NSSDC) trapped radiation models calculate the integral and differential electron and proton flux for given values of particle energy E, drift shell parameter L, and magnetic field strength normalized to the equatorial/minimum value on the field line B/B_0 for either solar maximum or solar minimum conditions. The most recent versions of the series of models, which have been developed and continuously improved over several decades by Vette and co-workers at NSSDC, are AE-8 for electrons and AP-8 for protons. The paper provides a brief history of the modeling efforts at NSSDC and discusses some of the problems encountered when applying the models at low altitudes. Recommendations are made and discussed about the correct use of the trapped particle models in conjunction with geomagnetic field models. Specifically, the importance of using the correct dipole moment and the correct B_0 value (i.e., obtained by field line tracing) is illustrated.

Introduction

SINCE the trapped radiation belts were first discovered by Van Allen[1] in 1958, it has been recognized that they are an important consideration in space flight because they can cause interference with scientific measurements, saturation of scientific instruments, damage to materials, and serious biological hazards to humans. In addition, high energy protons can undergo nuclear interactions, causing single event upset processes that generate soft errors in electronic components, such as memories and microprocessors. The low altitude region of the radiation belts is of particular interest because of the Shuttle and space station.

To evaluate the radiation exposure quantitatively, accurate models of the trapped radiation are necessary. The purpose of this paper is to describe the trapped particle models that have been developed at the National Space Science Data Center (NSSDC) and to discuss their limitations and the precautions necessary when applying the models. It is organized as follows. The next five sections provide a brief review of the history and properties of the models based largely on the more extensive report[2] compiled by Vette, the principal author of all of these models. Then certain limits of the validity of the models are discussed followed by the discussion and summary section. Availability of the model software is addressed in the concluding section.

Historical Review of the Trapped Particle Models

To understand the present status of the trapped particle models, it is useful to review the history of their development. In this section, such a review is given, concluding with the current models, AE-8 for electrons and AP-8 for protons.

In the early days of space research, there was no standard for the trapped particle environment. Consequently, each user took the existing data, extrapolated them in energy and space, and interpreted them for his or her needs. As a result of this, each design study or proposal that was submitted to NASA or to the Air Force had a different radiation environment, and within the ensemble of proposals for a particular project, the radiation environment assumed typically differed by a factor of 100. Since the radiation environment assumed affected the choice of orbits, the spacecraft shielding requirements, and the useful lifetime of the instruments, these differences in the radiation environment made it difficult to compare proposals.

The first models of the trapped particles were constructed at the NASA Goddard Space Flight Center (GSFC) by Hess, who started correlating various sets of data from the inner radiation belt after the Starfish nuclear explosion of July 9, 1962. These first models were unsophisticated compared to those available today, and they required a great deal of time and effort to translate the various data sets into a common parameter space. It soon became apparent that modeling the trapped particles was a fulltime job. In March 1964 Vette at the Aerospace Corporation was selected to receive joint NASA and Air Force funding to construct models of the electron and proton environments using the data acquired by various satellites. The modeling activity was transferred to GSFC in 1967 when Vette became the director of the National Space Science Data Center. This long-term project has produced eight electron models and eight proton models, which are the subjects of this paper.

Electron Models

The first electron model, AE-1,[3] treated the inner zone from L = 1.2 to 3 and energy E from 0.3 to 7 MeV. The data were organized with the B, L coordinate system of McIlwain[4] that the experimentalists used in their data analysis. The magnetic field model of Jensen and Cain[5] with an epoch of 1960 was applied for most of the data on which the AE and AP models are based. AE-1 was assigned an epoch of July 1963, but no specific decay model for the electrons from the Starfish nuclear explosion was given. The largest difficulties in producing AE-1 were the conversion of directional flux to omnidirectional flux and differential energy spectra to integral energy spectra, the determination of the threshold energy values for the instruments, and the translation of the data to the selected epoch using decay factors that were uncertain.

The second electron model AE-2[6] treated the inner zone electrons in a manner similar to AE-1 and for the first time also treated the outer zone electrons. The spatial range was from L = 1.1 to 6.3, which is just below the region of geostationary satellites. The energy range was from E = 0.04 to 7 MeV, and an epoch of August 1964 was assigned. Although the decay times from the Starfish electrons in the inner zone were known more accurately by this time, the Starfish effect was not considered in constructing AE-2. In the outer zone, magnetic storms cause rapid two to three orders of magnitude increases in the electron fluxes. These variations are not included in the model which represents time averages of the logarithm of the electron flux over periods of six months and more.

Presented as Paper 90-0176 at the AIAA 28th Aerospace Sciences Meeting, Reno, NV, Jan. 8–11, 1990; received Sept. 18, 1992; revision received March 12, 1993; accepted for publication March 12, 1993.

*Scientist, NSSDC Contract. Member AIAA.
†Section Manager, NSSDC Contract, 7601 Ora Glen Drive.

Table 1 NASA/NSSDC Trapped Radiation Models

Name	Energy Range (MeV)	L Range	Epoch	Ref.	Comments
Electrons					
AE-1	0.3–7	1.2–3	7/63	3	starfish not cons.
AE-2	0.04–7	1.1–6.3	8/64	6	
AE-3	0.01–5	6.6		7	geostationary
AE-4	0.04–4.85	3–11	1964/67	8	solar max. and min.
AE-5	0.04–4	1.2–2.8	10/67	9	starfish removed
AE-5P	0.04–4	1.2–2.8	1964	10	AE-5, solar min.
AE-6	0.04–4	1.2–2.8	1967	11	AE-5, solar max.
AE-8	0.04–7	1.2–11	1964/67	12	
Protons					
AP-1	30–50	1.17–4.6	9/63	3	
AP-2	15–30	1.17–3.5	9/63	3	
AP-3	>50	1.17–3.15	9/63	3	
AP-4	4–15	1.17–2.9	9/63	3	
AP-5	0.1–4	1.2–6.6		13	geost. inc.
AP-6	4–30	1.2–4	12/64	14	
AP-7	>50	1.15–3	1/69	15	as AP-3; sol. max.
AP-8	0.1–400	1.15–6.6	1964/70	16	solar min. and max.

The third electron model, AE-3,[7] treated the electron fluxes in the region of geostationary satellites $L = 6.6$. Instead of the coordinate B, the coordinate B/B_0 (with B_0 being the equatorial value on the magnetic field line) was used to measure the angular distance from the equator. The energy range was from 0.01 to 5 MeV. Solar cycle effects were not included because they were found to be smaller than the measurement errors. An important result was that the cumulative probability that the observed flux at a particular time would exceed a selected value could be approximated by a log normal distribution with an energy dependent standard deviation. This provided a powerful method of handling the time behavior if coherent effects were neglected.

The fourth electron model, AE-4,[8] treated the spatial region L = 3–11 and the energy range from 0.04 to 4.85 MeV. Two epochs were assigned, 1964 for solar minimum and 1967 for solar maximum. Solar cycle effects were introduced only in the region $L = 3$–5. An analytical low altitude cutoff was used because the data were incomplete in this region. The local time function was provided down to $L = 5$. For lower L values, no local time dependence could be found in the data. Using the same statistical approach as for AE-3 energy dependent standard deviations were provided. Only local time averaged fluxes were supplied with the computer code version.

The fifth electron model, AE-5,[9] treated the inner zone from L = 1.2 to 2.8. It was merged with AE-4 in the spatial region $L = 2.6$–2.8. The energy range was from 0.04 to 4.0 MeV. AE-5 was given the epoch of October 1967 (near solar maximum). This model was considerably more complex than the preceding electron models. The model treated three time effects: magnetic substorms, Starfish decay, and the solar cycle. For electron energies less than 0.7 MeV the solar cycle variation was the most important temporal effect. For intermediate energies near 1 MeV, the Starfish residue was significant at low L values. For energies greater than 0.7 MeV, substorm effects were studied at higher L values, but this effect was not included in the final model. AE-5 was the first model that was developed in directional flux and then converted to omnidirectional flux and could provide differential energy spectra as well as integral energy spectra.

The AE-5 1975 projected model[10] was obtained from AE-5 by adjusting the solar cycle dependence to correspond to solar minimum and by removing the Starfish residue. This made the AE-5 1975 projected model a companion to the epoch 1964 AE-4 model.

To obtain the electron model for the next solar maximum (AE-6[11]) the Starfish residue was removed from AE-5. Thus, it could be combined with the epoch 1967 AE-4 model to represent the electron distribution at solar maximum.

The electron models AE-I7 Hi and AE-I7 Lo were issued on an interim basis and were later withdrawn from circulation when it was determined that AE-I7 Hi was based on an erroneous analysis.

Current Electron Model

AE-8[12] is the current NSSDC electron model. It treats the spatial region from $L = 1.2$ to 11. In the inner zone it covers the energy range from 0.04 to 4.5 MeV, and in the outer zone the energies range from 0.04 to 7.0 MeV. The model is distributed in two versions, AE-8 MIN for solar minimum and AE-8 MAX for solar maximum. These models are a synthesis of three previous models (AE-5 1975 Projected, AE-4 epoch 1964 for solar minimum, and AE-6 and AE-4 epoch 1967 for solar maximum) and more recent data from four satellites. The analytical low altitude cutoff used in AE-4 was replaced by an empirical low altitude cutoff in the AE-8 models, and the local time dependence was extended down to L = 3. An additional improvement over AE-4 was made in the interface between the inner and outer zones in the region $L = 2.5$–2.9. The basic model that is distributed is a matrix of omnidirectional integral electron fluxes as a function of energy E, B/B_0, and L. Like its predecessors, AE-8 is a static model with the local time variation being averaged out. Figure 1 (from the AE-8 report[12]) shows the equatorial electron fluxes obtained from AE-8 as a function of L for various energies and solar maximum and minimum. Finally, the most important features of all of the electron models are summarized in Table 1..

Proton Models

The buildup and format of the proton models is similar to that of the electron models. The first four proton models covered the energy intervals 4–15 MeV (AP-4[3]), 15–30 MeV (AP-2[3]), 30–50 MeV (AP-1[3]), and energies greater than 50 MeV (AP-3[3]). By dividing the energy range into intervals, it was possible to represent the integral spectrum as exponentials with parameters that were functions of B and L. The epoch for the models was chosen to be just before the magnetic substorm of September 23, 1963. It was anticipated that the solar cycle variation would be included in future models.

The next proton model, AP-5,[13] treated the spatial range L = 1.2–6.6 and the energy range 0.1–4.0 MeV. Protons below the 0.1 MeV limit were not considered; protons of such low energy are not very important in view of space radiation effects on humans and materials. An exponential energy spectrum was used to conform to the previous proton models. Time variations were not included.

The proton model AP-6[14] covered the spatial range L = 1.2 to 4.0 and the energy interval 4–30 MeV. The energy spectrum was

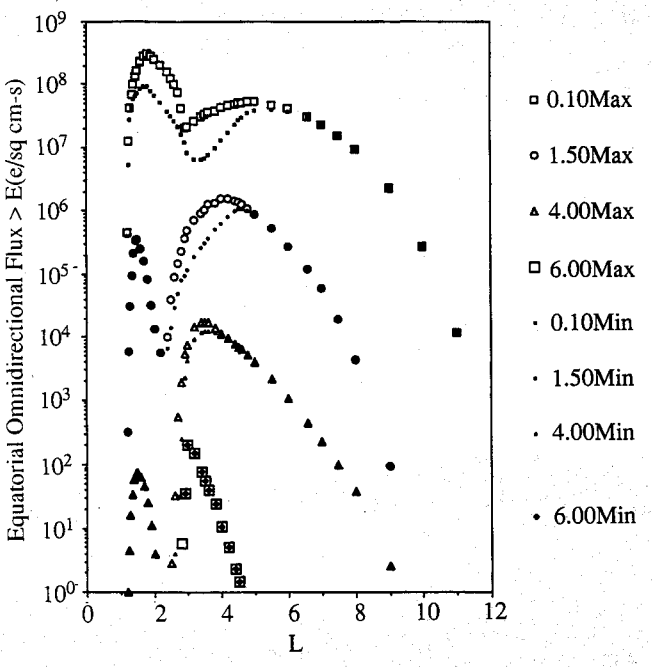

Fig. 1 L shell dependence of electron model fluxes.[11]

taken to be a power law rather than an exponential. Time variations were discussed in the documentation but not included in the model. An epoch of December 1964 was assigned to the AP-6 model.

The proton model AP-7[15] was an update of the AP-3 model for solar maximum conditions. An attempt was made to merge AP-1 and AP-3 into a single model for energies greater than 30 MeV. However, this was difficult to accomplish because the spectral functions for these two energy intervals had different spatial characteristics. The spatial region was from L = 1.15 to 3.0 and the epoch of the model was January 1969. The time variations were treated in the same way as those for AP-6.

Current Proton Model

AP-8[16] is the current NSSDC proton model. It treats the spatial region from L = 1.15 to 6.6 and the energy interval from 0.1 to 400 MeV. The model has two versions, AP-8 MIN for solar minimum with an epoch of 1964 and AP-8 MAX for solar maximum with an epoch of 1970. These models are a synthesis of the previous proton models AP-1 to AP 7, and the energy intervals have been merged smoothly. AP-8 is a static model except for the solar cycle variation. Time variations were discussed in the documentation but were not included in the model. Although the model was constructed in directional form, the basic model that is distributed is a matrix of omnidirectional integral proton fluxes as a function of energy B/B_0 and L. Figure 2 shows the equatorial proton fluxes as a function of L for various energies. Finally, the characteristics of all of the proton models are summarized in Table 1.

Limitations on the Validity of the Models

The AE and AP models are empirical, being based on data from in situ measurements of the fluxes of trapped particles; and like any empirical model, the models are as good as the data used in constructing them. In a number of cases a consensus had to be found, because of conflicting measurements and calibration inconsistencies. Comparisons of the models with data are provided in the documentation of the models to give users some estimate of the reliability. The errors associated with the models have been discussed in detail by Vette et al.[17] and Vette.[2,18] With the possible exception of where gradients are steep, it has been estimated that the models typically represent observed data within a factor of 2.

The second type of error that will be addressed results from using the models in a way that they were not intended to be used. The models of the trapped particle fluxes are based on in situ measurements performed in the 1960s and 1970s, and they were

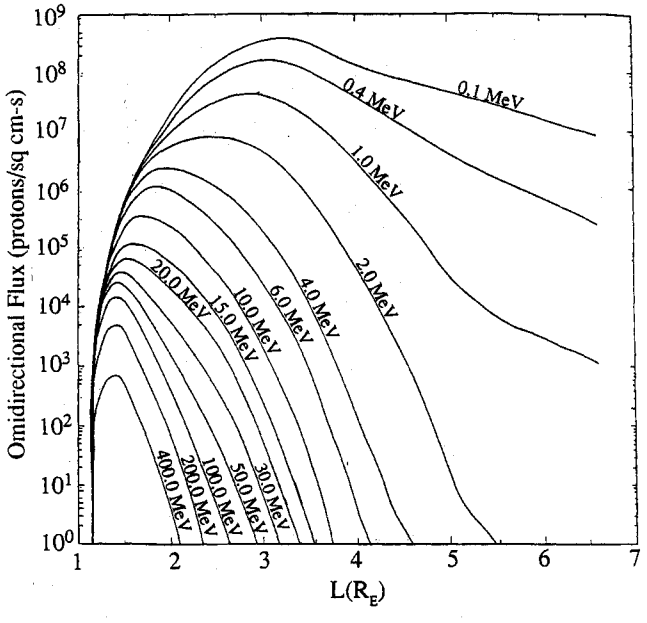

Fig. 2 L shell dependence of proton model fluxes.[16]

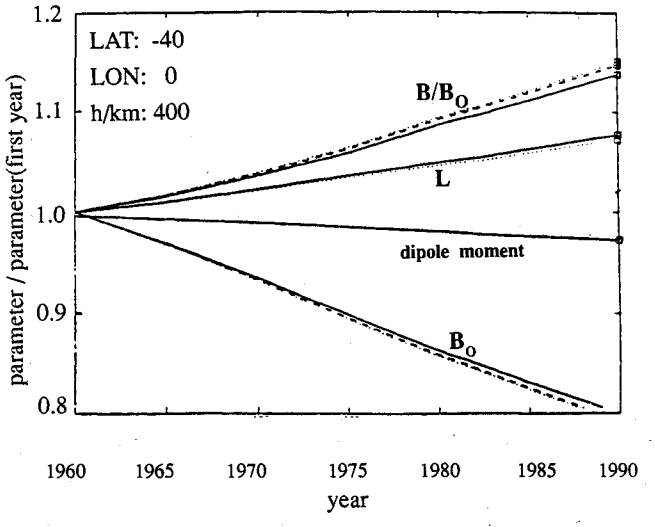

Fig. 3 Time evolution of B/B_0, L, magnetic dipole movement, and B_0; solid curves correspond to a fixed magnetic moment and B_0 calculated from dipole formula; dotted curves correspond to a magnetic moment calculated from IGRF field and B_0 calculated from dipole formula; dashed curves correspond to a dipole moment and B_0, both calculated from IGRF field.

adjusted to have an epoch in the 1960s or 1970. They were organized in magnetic field coordinates using the Jensen and Cain magnetic field model,[5] which has an epoch of 1960. When applying the models for a later epoch, one has to consider the secular variation of the Earth's magnetic field (the dipole moment is decreasing and the higher spherical harmonics are becoming relatively stronger). At present, the flux models are often used with the latest International Geomagnetic Reference Field (IGRF) magnetic field model,[19] which provides models for epochs from 1945, 1950, and so on until 1990. IGRF magnetic field models are issued by the International Association of Geomagnetism and Aeronomy (IAGA). IGRF models can be interpolated and extrapolated for a recommended maximum time period of five years. Some users[20,21] have had the need to estimate the radiation exposure for a low altitude, low inclination space station type orbit for the epochs 2000 to 2025. The geographical coordinates of the orbit (altitude, latitude, and longitude) were converted into magnetic coordinates B and L using a magnetic field model extrapolated into the 2000s. Fluxes were then calculated for these coordinates using the trapped particle models. It was found[20,21] that the models predicted an increase in particle fluxes by an order of magnitude or more as the epoch changed from the 1960s to the 2000s, depending on the type of particle, the energy, and the altitude of the orbit. To reduce this unrealistic and unwanted artifact of the models, Vette and Sawyer[22] made two recommendations. They suggested that users should provide B/B_0 instead of B as input for the computer code, and they recommended improvements in the computation procedure of the drift shell parameter L following a suggestion by Hilton[23] from a few years earlier. They noted that most L calculations were based on McIlwain's[4] pre-1960 fixed magnetic dipole moment that is hard coded into the often applied computer subroutine INVAR for calculating L. Instead, they suggested that L should be calculated with the magnetic dipole moment of the same epoch as the magnetic field model that is used to obtain the magnetic field strength B. With these modifications, both B/B_0 and L will be static in a collapsing dipole field. For the real (multipole) field, they will not be static but will change more slowly than in the case with the fixed dipole moment.

We have investigated the improvements resulting from the suggestion by Vette and Sawyer[22] for a number of locations. In addition to their L correction, we also investigated the effect of an improved determination of B_0. At present B_0 is obtained by assuming a magnetic dipole field; in this case the equatorial field strength B_0 is given by a simple formula. We have obtained the "real" B_0 by using a field line tracing procedure in the real multipole field

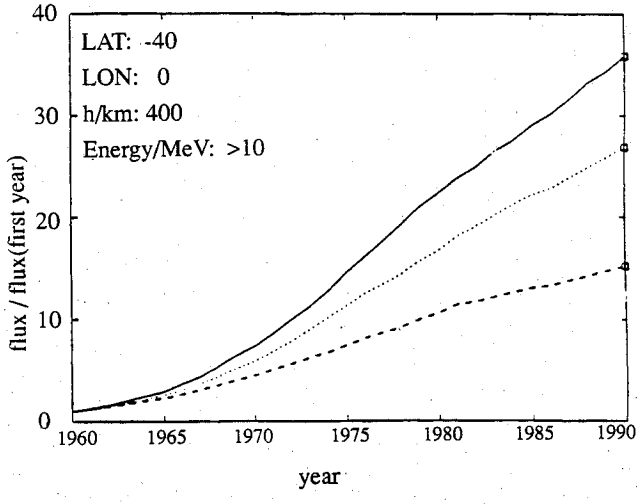

Fig. 4 Time evolution of the proton flux from AP-8MAX: solid curves correspond to a fixed magnetic moment and B_0 calculated from dipole formula; dotted curves correspond to a magnetic moment calculated from IGRF field and B_0 calculated from dipole formula; dashed curves correspond to a dipole moment and B_0, both calculated from IGRF field.

model. An example of our study results is shown in Fig. 3 for a position near the South Atlantic anomaly (SAA). The asymmetry of the Earth's magnetic field results in a region, the SAA, of very low magnetic field strength in the Atlantic ocean just off the northeastern coast of Brazil. At low altitudes the SAA is the only region where a low-inclination spacecraft (Shuttle, space station) encounters energetic protons. We considered a fixed position in space and calculated the magnetic coordinates B/B_0 and L for the epochs 1960 to 1990 using the IGRF magnetic field models for the corresponding epochs. Also shown in Fig. 3 are the magnetic dipole moment and B_0. In Fig. 3 three different ways of calculating the magnetic coordinates are indicated: 1) the solid lines were obtained by assuming a simple dipole field for the calculation of the minimum/equatorial field strength B_0 and by using a dipole moment fixed at McIlwain's[4] pre-1960 value for the L computation; 2) the dotted lines were obtained by calculating B_0 with the dipole formula as before, but by using the IGRF dipole moment for the L computation; and 3) the dashed lines were obtained by calculating B_0 as well as L for the particular IGRF field (B_0 is found by field line tracing in the IGRF field). All quantities are normalized to their value in the first year; except for the dipole moment, which is normalized to McIlwain's[4] pre-1960 fixed value.

Figure 3 shows that, as a result of the secular change in the magnetic field, B/B_0 and L increase, whereas the dipole moment and B_0 decrease. For comparison, we note that in a decreasing dipole magnetic field, the secular changes in the field are the same everywhere so that B/B_0 and L are constant. The effect of using the correct magnetic dipole rather than McIlwain's[4] fixed value is to slightly decrease L and B_0, and increase B/B_0. Calculating B_0 from the IGRF field rather than from a dipole field, on the other hand, raises B_0 again slightly. It is clear that the correct use of the geomagnetic field model in the L and B/B_0 calculation has only a minor compensating effect and does not provide near dipole-like behavior (i.e., almost constant L and B/B_0 over the 30-yr period). The corrections are about an order of magnitude smaller than the overall changes in L and B/B_0 over the 30-yr period.

The proton fluxes obtained from AP-8 MAX are plotted in Fig. 4 using the same cases and format as Fig. 3. There is a factor of 35 increase in the model proton flux from 1960 to 1990, as a result of the factor of 1.1 increase in L and B/B_0. Although the changes in B/B_0 and L are only of order of 10%, they produce changes in the flux that are more than an order of magnitude because the trapped particle model has very large gradients in this region of $B/B_0 \times L$ space. On a particular field line (i.e., L constant), we expect the trapped particle flux to decrease with increasing B/B_0. For constant B/B_0, on the other hand, the flux increases with increasing L because trapped particles on higher L shells have their mirror points higher in the atmosphere, where the neutral densities are lower and thus less particles are lost in collisions with neutrals. Both L and B/B_0 increase over the 30-yr time period and thus compensate each others' effect on the proton fluxes to a certain extent. However, the flux gradient vs L is much steeper than vs B/B_0, and the flux increase due to higher L values more than compensates the flux decrease due to higher B/B_0 values, resulting in an overall increase of the proton fluxes. Using the correct geomagnetic field parameters for the calculation of L and B/B_0 provides higher B/B_0 values and lower L values. Both of these changes produce reductions in the model proton fluxes. Overall the corrections result in a considerable lowering of the 30-yr factor from 35 to about 15. Because the trapped particle models are so sensitive to small changes in B/B_0 and L in this region, it is important to use the most accurate magnetic field model in calculating B/B_0 and L.

Discussion and Summary

The history of the development of the NSSDC trapped particle models leading up to the current proton model AP-8 and the current electron model AE-8 has been reviewed, and the difficulties encountered in developing the models have been discussed. The basic models that are distributed are matrices of omnidirectional, integral energy particle fluxes as a function of E, B/B_0, and L. Except for the solar cycle variation given by the two versions for solar maximum and minimum, these models are static; time variations have been averaged out. Greater detail on the history and problems of the trapped radiation model effort can be found in the reviews by the principal model author Vette,[2,18] and Vette et al.[17]

The effects of the secular decrease in the magnetic field model used in conjunction with the trapped particle models have been shown to produce large increases in the particle fluxes predicted for the future. Part of this increase was shown to result from using the magnetic field model inconsistently, i.e., using a fixed dipole moment when calculating L or using a dipole formula to calculate B_0. It should be also noted that the magnetic field models should not be extrapolated into the future for more than five years. Even if the magnetic field model is used consistently, smaller but significant increases in the fluxes still occur. The main reason for these increases is the fact that the decreasing magnetic field carries higher L shells to lower altitudes, and that the models do not take into account the increased atmospheric density the particles will encounter at lower altitudes. The use of the model maps with a magnetic field model/epoch different from the one used originally to generate the maps makes the inherently erroneous assumption that the trapped particle distribution is static with respect to the magnetic field and is carried along with the field as the field evolves. The particle distributions are, of course, dynamic and represent quasiequilibrium conditions. The time constants associated with the quasiequilibrium conditions are short compared to the time constant associated with the magnetic field evolution. Therefore, the evolving magnetic field has little effect on the spatial distribution of the particles. The primary effect is a change in the position of the South Atlantic anomaly region. Recently, Pfitzer[24] found that using the average atmospheric density at space station altitudes in the South Atlantic anomaly region as a variable in place of B/B_0 provides for a proper ordering of the AP-8 fluxes.

A look at the proton production and loss processes also does not indicate large increases in proton fluxes over time. An important source of the energetic protons and electrons at low L values is cosmic ray albedo neutron decay.[25] Because the particle loss time scales, in general, are short compared to the magnetic field decay time scale, no significant changes are expected in the trapped particle population as a result of the secular variation of the magnetic field. To avoid the prediction of artificial increases in particle fluxes over tens of years, it has been suggested[20–22] to use only the geomagnetic field models for the appropriate epochs, i.e., 1964 for solar minimum and 1970 for solar maximum. If the models are used with magnetic field models of later epochs, the effect of the increased atmospheric density should be taken into account.[24,26]

Availability of National Space Science Data Center Trapped Particle Models

The model software is available from NSSDC on tape, on diskette (for use on PCs), and online on computer networks (NSI-DECnet: NSSDCA:: REQUEST). The models can be also accessed and run online on the NSSDC Online Data and Information Service (NODIS) account: SET HOST NSSDCA, userid=NODIS, follow the menus. The software package includes an interactive driver program, the model coefficients and subroutines, and documentation files.

Acknowledgments

The authors acknowledge the support and guidance of J. Vette, J. King, and D. Sawyer, during the time this work was performed. Useful comments from the two referees resulted in significant improvements of this article.

References

[1]Van Allen, J. A., Ludwig, G. H., Ray, E. C., and McIlwain, C. E., "Observations of High Intensity Radiation by Satellites 1958 Alpha and Gamma," Jet Propulsion Lab. Rept. 558, Pasadena, CA, 1958.

[2]Vette, J. I., "The NASA/National Space Science Data Center Trapped Radiation Environment Model Program (1964-1991)," National Space Science Data Center, NSSDC/WDC-A-R&S, 91-29, Greenbelt, MD, Nov. 1991.

[3]Vette, J. I., "Models of the Trapped Radiation Environment—Vol. I: Inner Zone Protons and Electrons," NASA SP-3024, 1966.

[4]McIlwain, C. E., "Coordinates for Mapping the Distribution of Geomagnetically Trapped Particles," *Journal of Geophysical Research,* Vol. 66, Nov. 1961, pp. 3681–3691.

[5]Jensen, D. C., and Cain, J. C., "An Interim Geomagnetic Field," *Journal of Geophysical Research,* Vol. 67, No. 9, 1962, p. 3568.

[6]Vette, J. I., Lucero, A. B., and Wright, J. A., "Models of the Trapped Radiation Environment—Vol. II: Inner and Outer Zone Electrons," NASA, SP-3024, 1966.

[7]Vette, J. I., and Lucero, A. B., "Models of the Trapped Environment—Vol. III: Electrons at Synchronous Altitude," NASA SP-3024, 1967.

[8]Singley, G. W., and Vette, J. I., "The AE-4 Model of the Outer Radiation Zone Electron Environment," National Space Science Data Center, NSSDC/WDC-A-R&S 72-06, Greenbelt, MD, Aug. 1972.

[9]Teague, M. J., and Vette, J. I., "The Inner Zone Electron Model AE-5," National Space Science Data Center, NSSDC/WDC-A-R&S 72-10, Greenbelt, MD, Nov. 1972.

[10]Teague, M. J., and Vette, J. I., "A Model of the Trapped Electron Population for Solar Minimum," National Space Science Data Center, NSSDC/WDC-A-R&S 74-03, Greenbelt, MD, April 1974.

[11]Teague, M. J., Chan, K. W., and Vette, J. I., "AE-6: A Model Environment for Trapped Electrons for Solar Maximum," National Space Science Data Center, NSSDC/WDC-A-R&S 76-04, Greenbelt, MD, May 1976.

[12]Vette, J. I., "The AE-8 Trapped Electron Model Environment," National Space Science Data Center, NSSDC/WDC-A-R&S 91-24, Greenbelt, MD, Nov. 1991.

[13]King, J. H., "Models of the Trapped Radiation Environment—Vol. IV: Low Energy Protons", NASA SP-3024, 1967.

[14]Lavine, J. P., and Vette, J. I., "Models of the Trapped Radiation Environment—Vol. V: Inner Belt Protons," NASA SP-3024, 1969.

[15]Lavine, J. P., and Vette, J. I., "Models of the Trapped Radiation Environment—Vol. VI: High Energy Protons," NASA SP-3024, 1970.

[16]Sawyer, D. M., and Vette, J. I., "AP-8 Trapped Proton Environment for Solar Maximum and Solar Minimum," National Space Science Data Center, NSSDC/WDC-A-R&S 76-06, Greenbelt, MD, Dec. 1976.

[17]Vette, J. I., Chan, K., and Teague, M. J., "Problems in Modeling the Earth's Trapped Radiation Environment," Air Force Geophysical Lab., AFGL-TR-78-0130, Hanscom AFB, MA, Jan. 1978.

[18]Vette, J. I. "Trapped Radiation Models," *Development of Improved Models of the Earth's Radiation Environment,* MATRA-ESPACE, Tech. Note 1 Model Evaluation, Toulouse, France, June 1989.

[19]Anon., "IGRF, Revision 1987," *Journal of Geomagnetism and Geoelectricity,* Vol. 39, No. 12, 1987, p. 773.

[20]Konradi, A., Hardy, A. C., and Atwell, W., "Radiation Environment Models and the Atmospheric Cutoff," *Journal of Spacecraft and Rockets,* Vol. 24, No. 2, 1987, pp. 284, 285.

[21]Daly, E. J., "Effects of Geomagnetic Field Evolution on Predictions of the Radiation Environment at Low Altitudes," European Space Agency, ESTEC Working Paper 1531, Noordwijk, The Netherlands, Jan. 1989.

[22]Vette, J. I., and Sawyer, D. M., "Short Report on Radiation Belt Calculations," unpublished, 1986.

[23]Hilton, H. H., "*L* Parameter, A New Approximation," *Journal of Geophysical Research,* Vol. 76, No. 28, 1971, pp. 6952, 6953.

[24]Pfitzer, K. A., "Radiation Dose to Man and Hardware as a Function of Atmospheric Density in the 28.5° Space Station Orbit," McDonnell-Douglas Space Systems Co., Rept. H5387A, Huntington Beach, CA, March 1990.

[25]White, R. S., "High-Energy Proton Radiation Belt," *Reviews in Geophysics and Space Physics,* Vol. 11, No. 3, 1973, p. 595.

[26]Lemaire, J., "Development of Improved Models of the Earth's Radiation Environment," Belgian Inst. of Space Aeronomy Final Rept., Brussels, Sept. 1990.

Alfred. L. Vampola
Associate Editor